83-1888

A COMPARATIVE STUDY OF THE NONUNIQUENESS PROBLEM OF THE POTENTIAL EQUATION

M. D. Salas*

NASA Langley Research Center
Hampton, Virginia

A. Jameson**

Princeton University
Princeton, New Jersey

R. E. Melnik+

Grumman Aerospace Corporation
Bethpage, New York

A83-39357

Abstract

The nonuniqueness problem occurring at transonic speeds with the conservative potential equation is reviewed. Additional evidence supporting the idea that the nonuniqueness problem is inherent to the differential equation is given. An extensive, comparative study between potential and Euler calculations is presented. The results of the study indicate that the nonuniqueness problem is not an inviscid phenomenon, but a result of the conservative potential approximate treatment of shock waves. A new bound on the limit of validity of the potential formulation is discussed.

Introduction

At the previous gathering of this conference 2 years ago, Steinhoff and Jameson[1] showed that the numerical solutions of the full-potential equation for flow past an airfoil are not unique. In the same paper, a meticulous study was conducted which indicated that the anomaly is inherent to the partial-differential equation and not a result of its discrete representation. Having reached this conclusion, the authors went on to conjecture on the possibility of the anomaly being an inviscid phenomenon, perhaps inherent to the more exact Euler equations and maybe a contributing factor in the occurrence of buffeting.

Given today's preeminent position of the potential approximation in the transonic range for the design and analysis of airfoil profiles, it is unnecessary to dwell on the importance of investigating the conjectures made in Ref. 1. That is the purpose of this paper. The paper is divided into three main parts. First, a brief review of Steinhoff/Jameson's study and some new findings made in the course of this work are presented. Second, the Euler code described in Ref. 2 is introduced and the improvements and validation procedure used to determine its accuracy are described. Finally, results from a comparative study of the nonuniqueness problem for the potential and Euler models are presented and discussed.

The results and conclusions in this paper supercede the preliminary results presented in Ref. 3.

Review of the Potential Anomaly

While introducing lifting capability to the full-potential, conservative, nonlifting, multigrid code described by Jameson in Ref. 4, Steinhoff[1] discovered that three converged solutions could be obtained for a symmetric airfoil at zero angle of attack, α, and fixed free-stream Mach number, M_∞. These solutions consisted of a zero-lift symmetric solution and two mirror-image asymmetric solutions with large absolute levels of lift. The latter two could be obtained by perturbing the zero-lift solution which was unstable. The multigrid capability of the code made it feasible to converge all three solutions to machine accuracy.‡ This unquestionably indicated the multiplicity of solutions of the discrete system of equations. In order to determine if the anomaly was characteristic of the partial-differential equation being modeled, the following tests were made in Ref. 1:

1. The solutions were checked to determine if they had the expected farfield decay corresponding to a vortex and a doublet in a uniform stream. They did. In addition, the effect of the location of the outer boundary was investigated. It slightly affected the lift level, but the nonuniqueness problem persisted.

2. Originally, the anomaly was observed for an airfoil with nonzero trailing-edge

*Research Scientist. Assoc. Fellow AIAA.

**Professor. Assoc. Fellow AIAA.

+Director of Fld. Mechanics. Assoc. Fellow AIAA.

‡Residuals of the order of 10^{-12} in a CDC CYBER 203 computer for the cases reported here.

angle. In order to determine the effect of imposing the Kutta condition, a Joukowski profile was investigated. The Joukowski profile, with its cusped trailing edge, requires a smooth matching of the pressures on the upper and lower surfaces. Again, the numerical solutions showed the proper behavior, but the anomaly persisted.

3. The convergence of the solution with mesh refinement was investigated using grids with 96x24, 128x32, 192x48, 256x64, and 384x192 cells. The solutions were found to change little with mesh refinement.

4. The effect of artificial viscosity was tested by using both first- and second-order accurate expressions for this term.

5. Since all the calculations were originally made with an "O" mesh defined by a conformal circle mapping, calculations using a "C" mesh were tried. The multiple solutions were observed with the "C" mesh.

6. Similar results were obtained with the conservative finite-difference, potential code described in Ref. 5.

In addition, during the course of the present investigation, we have found the following results:

7. The multiple solutions also occurred with the conservative potential code described in Ref. 6.

8. A standard feature of these codes (Refs. 4-6) is to require the reduced far-field potential, ϕ_F, to satisfy the leading term of the compressible vortex solution; namely:

$$\phi_F = \frac{\Gamma}{2\pi} \tan^{-1} (\beta \tan \theta) \qquad (1)$$

$$\beta = \left(1 - M_\infty^2\right)^{1/2} \qquad (2)$$

where θ is the polar angle and Γ is the value of the circulation that satisfied the Kutta condition. Because Γ evolved as part of the solution, it is reasonable to be suspicious of this boundary condition as a possible cause of the anomaly. To check this, calculations were made with the "wind-tunnel" code described in Ref. 7. In this code, the far-field boundary condition corresponds to no flow through the tunnel walls; that is

$$\left.\frac{\partial \phi_F}{\partial y}\right|_{y=\pm h} = 0 \qquad (3)$$

with $h = 50$ airfoil chords. The multiple solutions were also found with this code.

9. No multiple solutions were found with the nonconservative code described in Ref. 8 (FLO 12).

Although the above tests are not conclusive, they make a strong case for the argument that the problem exists at the differential level of the conservative potential formulation. Therefore, with no evidence to the contrary, we will proceed under that assumption.

An interesting feature of the results presented in Ref. 1 was the occurrence of a "gap" in the lift-α curve. The "gap" was explained in Ref. 1 in terms of a hysteresis effect. In this investigation, it was determined that the "gap" comes about because in this range of angles of attack the lift becomes a multivalued function of the angle of attack. The piece of the lift-α curve missing in Ref. 1 can easily be obtained by prescribing the lift and letting the numerical solution determine the angle of attack which satisfies the Kutta condition. In this manner, the complete lift-α curve for an NACA 0012 airfoil has been evaluated at $M_\infty = 0.83$ using a modified version of the code used in Ref. 1 (FLO 36). The results are shown in Fig. 1.

For the NACA 0012 airfoil, the results presented here show the anomaly occurring in the neighborhood of zero angle of attack. It should not be inferred from this that the anomaly occurs only in this narrow Mach number/angle-of-attack envelope. For example, for the NACA 0012 airfoil at $\alpha = 1^\circ$, it appears at $M_\infty \approx 0.79$; and at $\alpha = 9^\circ$, it appears at $M_\infty \approx 0.6$.

Also of interest is that the anomaly has been observed in the presence of a single shock for flow past an RAE 2822 profile at $M_\infty = 0.75$ and α of about 1°. The lift-α curve for these conditions is shown in Fig. 2. The single shock wave occurs on the upper surface.

Nonuniqueness is not new to potential theory. An incompressible flow past a lifting airfoil with a sharp trailing edge has a one-parameter family of solutions. In this case, the relevant physical solution is singled out by the Kutta condition. At supercritical speeds, solutions with "expansion" shocks are mathematically valid solutions of the governing differential equation. Expansion shocks are ruled out in favor of the physically relevant compression shock by invoking the Second Law of Thermodynamics. Why not resolve the present dilemma by imposing some new constraint? If we consider Fig. 1 again, it seems reasonable that for zero angle of attack the relevant solution is the symmetric solution corresponding to zero lift. Increase the angle of attack by a small amount. Which of the three solutions is the physically relevant solution? The two with the largest absolute levels of lift can be ruled out on the grounds that they require a discontinuous behavior as α goes to zero. However, the remaining solution does not seem physically relevant either; since it predicts negative lift at positive angle of attack. The nonuniqueness problem we are facing is unique in that none of

the solutions available seems to be physically relevant!

The question now is: Is this anomaly a problem of the potential approximation in the transonic range or a problem of the inviscid flow? To investigate this question, we propose to do a systematic search with an Euler flow code. But, before proceeding to this step, it is necessary to establish the validity of the numerical results of the Euler code. This is the next step in our investigation.

Improvements and Validation of FLO 52-S

The finite-volume, fourth-order Runge-Kutta code described in Ref. 2 was chosen for this study because of its fast convergence rate. The code solves the time-dependent continuity, x-momentum, y-momentum, and energy equations in conservation form. In order to prevent typical central-difference, odd-even oscillations; and, in order to capture shock waves, a blended fourth- and second-order explicit artificial damping term is added to the equations. To accelerate the rate of convergence, each mesh cell is advanced at its own local time step, Δt, and the governing equations are modified by an enthalpy damping term. The calculations were done using a nearly orthogonal "O" mesh with an inverse radial transformation to cluster mesh points near the airfoil. A detailed account of the discretization, damping, and acceleration technique is given in Ref. 2.

In its original version, for lifting subcritical calculations, the code consistently under-predicted the lift coefficient predicted by potential calculations by as much as 10 percent. In addition, isomach plots revealed a disturbing behavior near the airfoil surface. As the isomach lines approached the surface, they turned abruptly indicating an incorrect "boundary-layer" like behavior. This was also evident in flow-field plots of entropy and total pressure losses.

The cause of the problem was found to be associated with the evaluation of the damping terms near the airfoil surface and in the far field. As described in Ref. 2, the damping term is made up of contributions in the two coordinate directions X and Y with associated indexes i,j, respectively. Let X be the coordinate along an "O" ring and Y in the other direction. The damping term is given by

$$Dw = D_X w + D_Y w \tag{4}$$

$$D_X w = d_{i+1/2,j} - d_{i-1/2,j} \tag{5}$$

$$D_Y w = d_{i,j+1/2} - d_{i,j-1/2} \tag{6}$$

with w being the vector of unknowns and a typical d term defined by

$$d_{i,j+1/2} = \frac{h_{i,j+1/2}}{\Delta t}\left[\varepsilon^{(2)}_{i,j+1/2}\Delta w_{i,j+1/2} - \varepsilon^{(4)}_{i,j+1/2}\left(\Delta w_{i,j+3/2} - 2\Delta w_{i,j+1/2} + \Delta w_{i,j-1/2}\right)\right] \tag{7}$$

where h is the cell area, $\varepsilon^{(2)}$ and $\varepsilon^{(4)}$ are coefficients, defined in Ref. 2, which depend on the second derivative of pressure and

$$\Delta w_{i,j+1/2} = w_{i,j+1} - w_{i,j} \tag{8}$$

The evaluation of the d terms presents some problems near the airfoil surface, $j \leq 2$, and near the last "O" ring, $j > J_{max}-1$, because of the lack of information near these cells. In the original code, Δw terms inside the airfoil and outside the last "O" ring were constructed using a third-order extrapolation from inside the flow field.

The "boundary-layer" like behavior was eliminated by the following procedure. At a ghost point, j=0, inside the airfoil, the pressure, density, and total enthalpy were obtained by linear extrapolation from inside the flow field. The velocity components at the cell center immediately next to the airfoil surface were decomposed into components normal and tangent to the surface. These were then reflected to obtain components at the ghost cell. With this information, it was possible to evaluate

$$\Delta w_{i,1/2} = w_{i,1} - w_{i,0}.$$

The missing term, $\Delta w_{i,-1/2}$, was evaluated by equating it to $\Delta w_{i,1/2}$. Although this procedure eliminated the "boundary-layer" behavior, it had little effect on the low-lift level being predicted. Surprisingly, the problem with the lift was corrected by modifying the evaluation of the far field damping terms. The finite volume integration is performed only up to $J_{max}-1$; values of w at J_{max} are obtained by satisfying the far-field boundary conditions, which use no damping. Therefore, to evaluate the damping terms at $J_{max}-1$, only additional information for the term $\Delta w_{i,J_{max}+1/2}$ is required. When this term was approximated by

$$\Delta w_{i,J_{max}+1/2} = \Delta w_{i,J_{max}-1/2},$$

the error in the lift level was reduced to about 1 percent.

The far-field boundary condition evaluation in the original code used the method of Rudy and Strickwerda[9] which introduces an additional free parameter into the calculation. This method was

replaced by the following procedure which proved more robust and made a slight improvement in the convergence rate. At a subsonic point, a frame of reference perpendicular and tangential to the last "O" ring is constructed. In the plane made by the perpendicular to the "O" ring and the time axis, the Riemann "invariant" that propagates along the characteristic coming into the computational region is prescribed from known free-stream values. The Riemann "invariant" propagated by the outgoing characteristic is extrapolated from computed values. From these two quantities the speed of sound and the velocity component normal to the "O" ring are determined. If the point corresponds to an inflow point, the entropy and velocity components tangent to the "O" ring are prescribed from free-stream values. If the point corresponds to an outflow point, the entropy and velocity components tangent to the "O" ring are extrapolated from computed values. From these four quantities, the conservative unknown vector w is evaluated.

For supersonic inflow, all quantities are prescribed; while for supersonic outflow, all quantities are extrapolated from computed values.

The code was also modified to include, as an option, the effect of a far-field vortex. To this end, the circulation is approximated from the lift calculated by the integration of the surface pressure. Then, the free-stream Cartesian velocity components, u_∞ and v_∞, are replaced, to account for the vortex, by

$$\bar{u}_\infty = u_\infty + \kappa \sin(\theta - \alpha) \tag{9}$$

$$\bar{v}_\infty = v_\infty - \kappa \cos(\theta - \alpha) \tag{10}$$

where

$$\kappa = \frac{\left(u_\infty^2 + v_\infty^2\right)^{1/2} \beta\Gamma}{2\pi r\left(1 - M_\infty^2 \sin^2(\theta - \alpha)\right)} \tag{11}$$

and where r, θ are polar coordinates in the physical plane with origin at the center of the airfoil. The free-stream thermodynamic variables are recomputed using the magnitude of free-stream velocity given by Eqs. (9) and (10), the steady-state Bernoulli's equation, and the known value of entropy at the point in question. In general, the far-field vortex had very little effect on the calculated results. This is probably due to the location of the last "O" ring which in these calculations corresponded to about 100 chords from the airfoil.

The last major modification to the Euler code consisted of a second-order accurate integration of the normal pressure gradient at the surface of the airfoil to evaluate the surface pressure. As discussed in Ref. 2, because of the finite volume formulation and the fact that the fluxes convected across the airfoil surface are zero, only the pressure needs to be evaluated at the surface. In this connection, it should be stressed that the evaluation of ghost points, discussed in relation to the damping terms, has nothing to do with the evaluation of the surface boundary conditions.

For reference purposes, we will designate the modified Euler code as FLO 52-S. A large number of lifting subcritical cases were calculated with this code using a 120x34 mesh and with the potential code FLO 36 using a 192x32 mesh. Due to space limitations, results are presented for only one of the "worst" subcritical lifting cases computed--an NACA 0012 airfoil at $M_\infty = 0.3$ and $\alpha = 10^\circ$. A partial view of the mesh corresponding to 120x34 points is shown in Fig. 3. Fig. 4 shows that second-order accuracy in the lift and drag coefficients is attainable with mesh refinement. Fig. 5 shows a typical convergence behavior. The residuals plotted in Fig. 5(a) are the root mean squares of $\frac{\Delta\rho}{\Delta t}$, $\frac{\Delta\rho u}{\Delta t}$, and $\frac{\Delta\rho v}{\Delta t}$ evaluated over the entire field. Fig. 5(b) shows the convergence of lift, drag, and moment coefficient, each evaluated from the integration of the surface pressure. A comparison between FLO 36 and FLO 52-S for the surface pressure distribution, isomach contours, and streamline trajectories is shown in Figs. 6-8. Practically no difference can be observed if the results of the two calculations are overlaid; we emphasize that this represents the "worst" case computed.

At supercritical speeds, the potential calculations are only approximate solutions to the inviscid flow. Typically, these calculations have a stronger shock wave which appears further aft than in Euler calculations. Two typical results at $M_\infty = 0.82$ and 0.84--both at zero angle of attack--are shown in Figs. 9 and 10. A check on how well the shock wave is captured is shown in Fig. 11 where the calculated shock jump is compared to the exact jump. Taking into consideration the difficulty in reading the results because of the shock-wave smearing and the Zierep singularity, the agreement is quite good. For comparison, the results of the nonconservative potential code, FLO 12, are also included.

Nonuniqueness Study

The lift-α curve shown in Fig. 1 is repeated in Fig. 12; but, in the latter, the results of the Euler calculation and the nonconservative potential code FLO 12, are also included. As can be seen from this figure, the Euler results do not show any anomaly at this particular Mach number. Can it be that the Euler solution will be anomalous at some other Mach number? In order to study this, consider the angle made by the lift-α curve with the abscissa at zero lift. If this angle exceeds 90°, then we are in the anomalous region where a positive angle of attack produces negative lift. Fig. 13 shows the behavior of this angle as a function of free-stream Mach number for conservative potential, nonconservative potential, and Euler. The figure shows that the conservative potential solution becomes progressively worse as the free-stream Mach number increases, eventually crossing over into the multiple solution region at about $M_\infty = 0.82$. Both the Euler solutions and the nonconservative solutions remain well-behaved throughout the Mach number range. The anomaly,

therefore, is indicative of a breakdown of the conservative potential formulation.

In Fig. 14, the same plot of Fig. 13 is repeated in terms of transonic similarity parameters.[10] It is interesting to see that the conservative potential results are reduced to a single curve in the similarity plane. This is another indication that the numerical code is predicting the expected behavior of the partial-differential equation. It furthermore indicates that the nonuniqueness problem will occur even for very weak shock waves if the airfoil thickness, τ, is made sufficiently small. The fact that the Euler results do not collapse into a single curve in the similarity plane is not unexpected, since the similarity law is only valid for the small-disturbance potential equation. The rapid drop in lift shown in Fig. 14 for $\chi < 0.8$ has been explained as an inviscid phenomenon associated with the inefficient production of lift that occurs when the upper surface shock wave moves to the trailing edge.[10,11]

Something else can be inferred from Fig. 14. Classically, potential theory is accepted as a good approximation in the transonic range to the rotational inviscid flow if the shock is weak. The shock strength is measured by $M_s^2 - 1$, where M_s is the Mach number in front of the shock. The rationale is based on the fact that the entropy produced at the shock is proportional to the cube of the shock strength. Thus, the potential approximation is accepted if

$$\left(M_s^2 - 1\right)^3 \ll 1 \qquad (12)$$

However, the results of Fig. 14 seem to say something else. Two potential flows are topologically equivalent for affine airfoil profiles if they have the same transonic similarity parameter χ. It will be reasonable to expect that if one of these flows violates the criterion defined by Eq. (12), the other flow will also violate this criterion. This is not the case, since Eq. (12) is not scaled according to similarity rules. If we rewrite Eq. (12) in terms of a similarity scaled entropy we get

$$\left(M_s^2 - 1\right)^3 \ll \tau^2 \qquad (13)$$

which seems to be a more reasonable criterion for the validity of potential theory. This, however, severely limits the transonic region for which the potential theory represents a valid approximation to an inviscid rotational flow.

A heuristic explanation for the conservative potential anomaly can be arrived at if we consider a quasi-one-dimensional nozzle flow. With the nozzle choked, two isentropic solutions are possible--one corresponding to subsonic flow, the other corresponding to supersonic flow. Of these two, the one that appears is determined by matching the downstream pressure. If a downstream value of pressure is prescribed between these two extremes, a shock wave forms in the divergent part of the nozzle. The position of the shock is established by matching the prescribed downstream pressure. The above description is properly modeled by the Euler equations. What happens if the problem is described by the conservative potential equation? If the downstream value of pressure corresponds to the subsonic isentropic solution, a solution with supersonic flow downstream of the throat followed by an isentropic compression shock is still possible; since this solution will satisfy the downstream boundary condition. Moreover, the shock can be placed anywhere downstream of the throat and still satisfy the differential equation and the boundary condition. The problem comes about because the exact isentropic jump is being satisfied and this jump connects the subsonic and supersonic isentropic branches. This is not the case with the Euler equations, because of the entropy produced at the shock; or with the nonconservative potential, because the exact isentropic jump is not satisfied. It is this weakness of the conservative formulation to fix the shock position in the quasi-one-dimensional problem which might be responsible for the anomaly observed in two dimensions. If this is the case, the nonuniqueness problem could be resolved by abandoning the isentropic, mass-conserving shock-wave formulation for some other shock representation; see, for example, Ref. 12. However, it seems that in order to retain a rational formulation, some form of shock-fitting will be required.

Conclusions

Additional evidence has been provided which supports the thesis of Ref. 1, that the nonuniqueness is a problem inherent to the conservative potential differential equation. The hysteresis effect proposed in Ref. 1 has been shown to be a numerical result due to the multivalue nature of the computed lift in a certain range of α.

None of the multiple solutions obtained with the conservative potential formulation seems to be relevant to the physical problem. Rather, they seem to indicate a breakdown of the theory. It appears that to avoid the anomaly the conservative formulation must be abandoned.

A more restrictive criterion for the validity of potential theory in the transonic range has been proposed. This criterion shows that shock-wave strength should be measured relative to airfoil thickness.

The numerical results obtained with the Euler code indicate that the nonuniqueness problem is not inherent to the inviscid solution. However, it is felt that more research is necessary to settle this issue conclusively. Finally, it is not known if the anomaly persists in three-dimensional flows or if it can be removed through interaction with a boundary layer.

Acknowledgment

Many members of the Theoretical Aerodynamics Branch, NASA Langley Research Center, contributed to this effort. The authors are especially

grateful to Mr. Clyde R. Gumbert who ran FLO 36 and to Mr. Jerry C. South, Jr., for his advice and encouragement.

References

[1]Steinhoff, J. and Jameson, A., "Multiple Solutions of the Transonic Potential Flow Equation," AIAA Paper No. 81-1019, Proceedings of the AIAA 5th Computational Fluid Dynamics Conference, Palo Alto, Calif., June 1981, pp. 347-353.

[2]Jameson, A., et al., "Numerical Solutions of the Euler Equations by Finite Volume Methods Using Runge-Kutta Time-Stepping Schemes," AIAA Paper No. 81-1259, AIAA 14th Fluid and Plasma Dynamics Conference, Palo Alto, Calif., June 1981.

[3]Salas, M. D., et al., "Non-Unique Solutions to the Transonic Potential Flow Equation," AIAA Technical Note. (To appear in AIAA J.)

[4]Jameson, A., "A Multi-Grid Scheme for Transonic Potential Calculations on Arbitrary Grids," Proceedings of the AIAA 4th Computational Fluid Dynamics Conference, Williamsburg, Va., July 1979, pp. 122-146.

[5]Bauer, F., et al., "Supercritical Wing Sections II," Springer-Verlag, New York, 1975.

[6]Dougherty, F. C., et al., "TAIR-A Transonic Airfoil Analysis Computer Code," NASA TM 81296, 1981.

[7]Doria, M. L. and South, J. C., Jr., "Transonic Potential Flow and Coordinate Generation for Bodies in a Wind Tunnel," AIAA Paper No. 82-0223, AIAA 20th Aerospace Sciences Meeting, Orlando, Fla., Jan. 1982.

[8]Jameson, A., "Iterative Solution of Transonic Flows Over Airfoils and Wings Including Flows at Mach 1," Commun. Pure & Appl. Math., Vol. 27, No. 3, May 1974, pp. 283-309.

[9]Rudy, D., and Strikwerda, J., "A Non-reflecting Outflow Boundary Condition for Subsonic Navier Stokes Calculations," J. Comp. Phys., Vol. 36, 1980, pp. 55-70.

[10]Cole, J. D., et al., "Transonic Flow Past Simple Bodies," J. Aeronaut. Sci., Vol. 20, No. 9, 1953, pp. 627-634.

[11]Mair, W. A. and Beavan, J. A., "Flow Past Airfoils and Cylinder," Modern Developments in Fluid Dynamics - High Speed Flow," Vol. II, L. Howarth, ed., Clarendon Press, Great Britain, 1953, p. 656.

[12]Klopfer, G. H. and Nixon, D., "Non-Isentropic Potential Formulation for Transonic Flows," AIAA Paper No. 83-0375, AIAA 21st Aerospace Sciences Meeting, Reno, Nev., Jan. 1983.

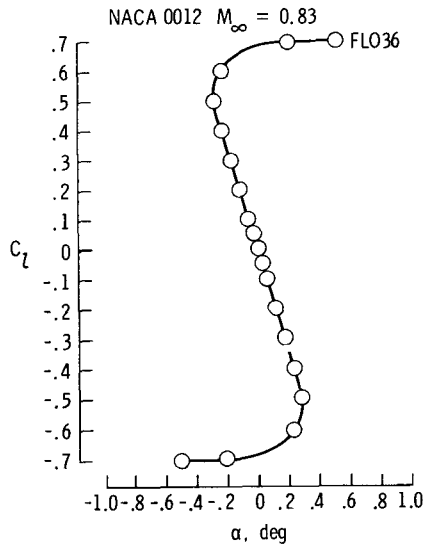

Fig. 1.- Lift-α curve obtained with FLO 36 for an NACA 0012 airfoil.

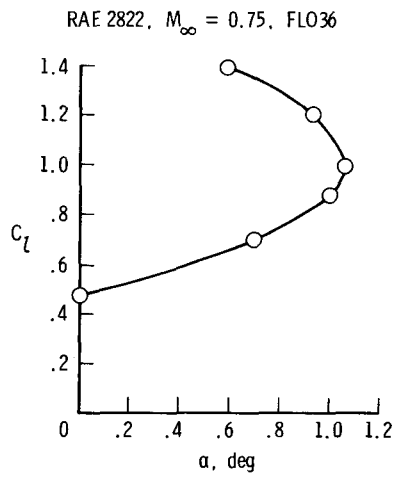

Fig. 2.- Lift-α curve obtained with FLO 36 for an RAE 2822 airfoil.

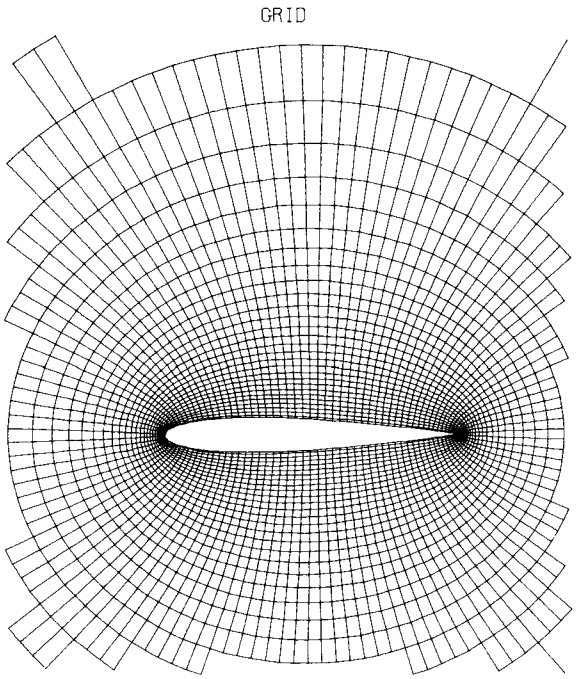

Fig. 3.- Partial view of mesh used in FLO 52-S.

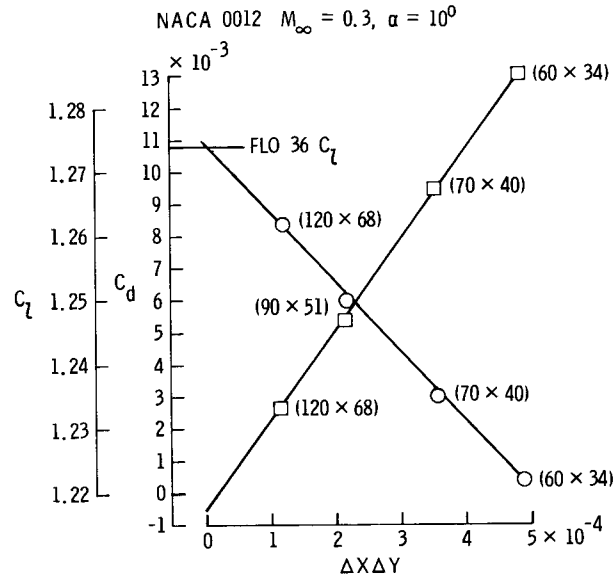

Fig. 4.- Convergence of lift (circles) and drag (squares) coefficients with mesh refinements.

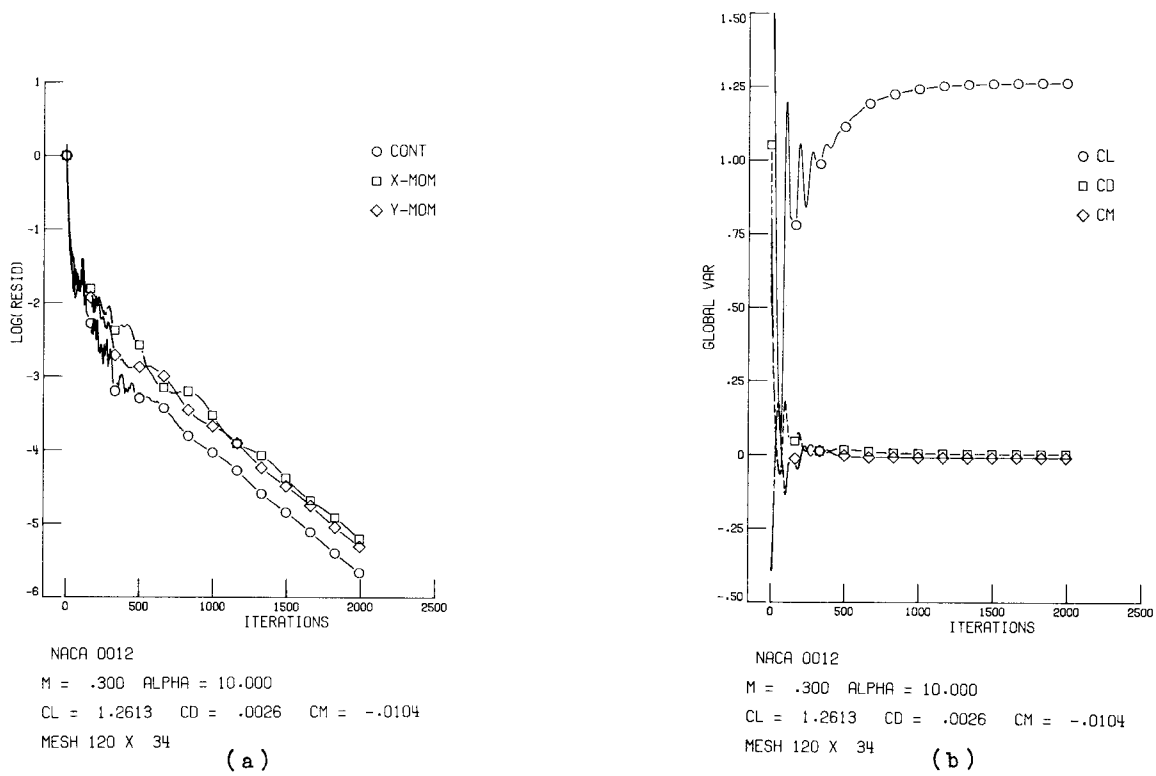

Fig. 5.- Convergence histories for (a) residual decays and (b) lift, drag and moment coefficients.

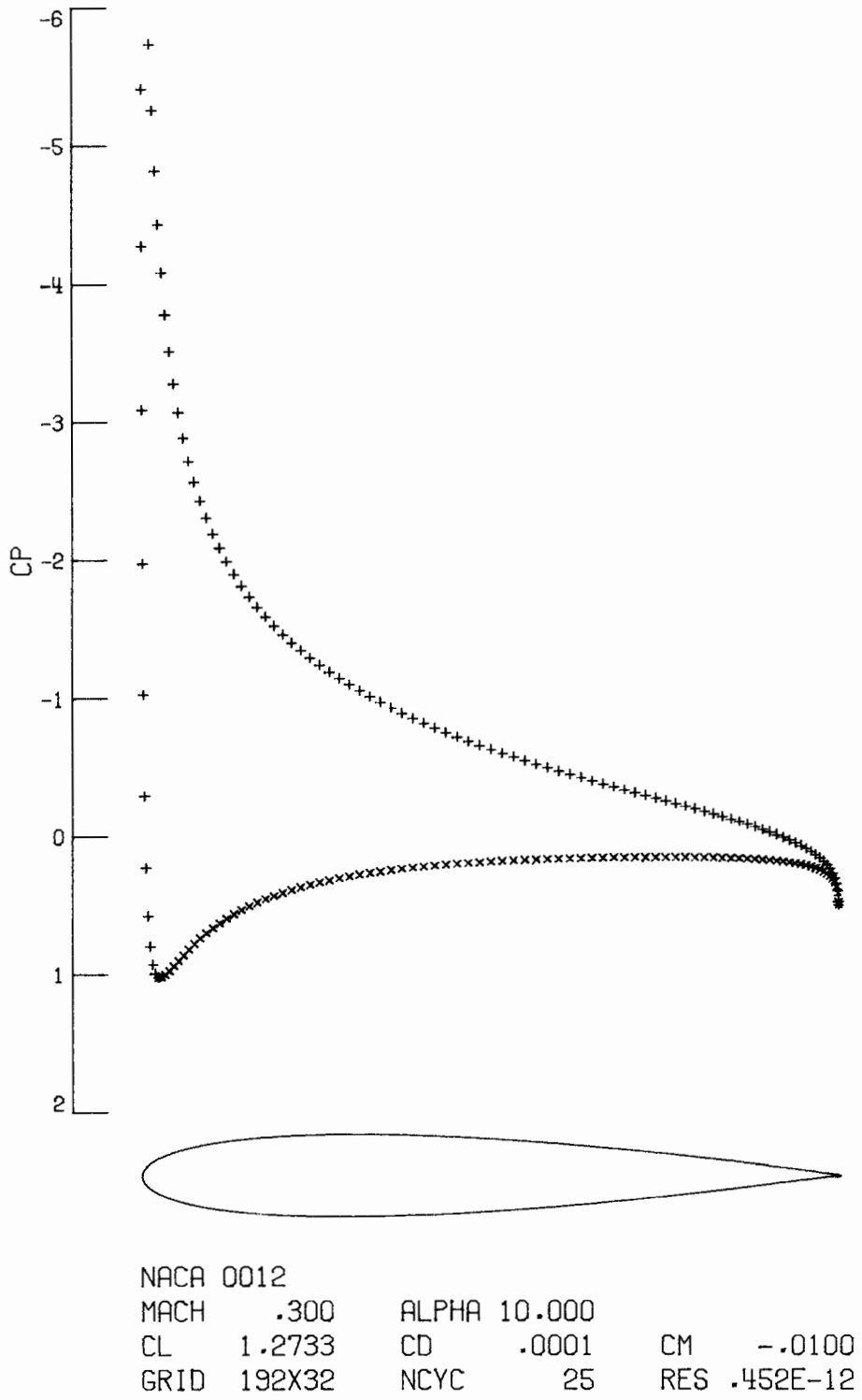

(a)

Fig. 6.- Pressure coefficient computed for an NACA 0012 airfoil at $M_\infty = 0.3$, $\alpha = 10^\circ$ with (a) FLO 36 and (b) FLO 52-S.

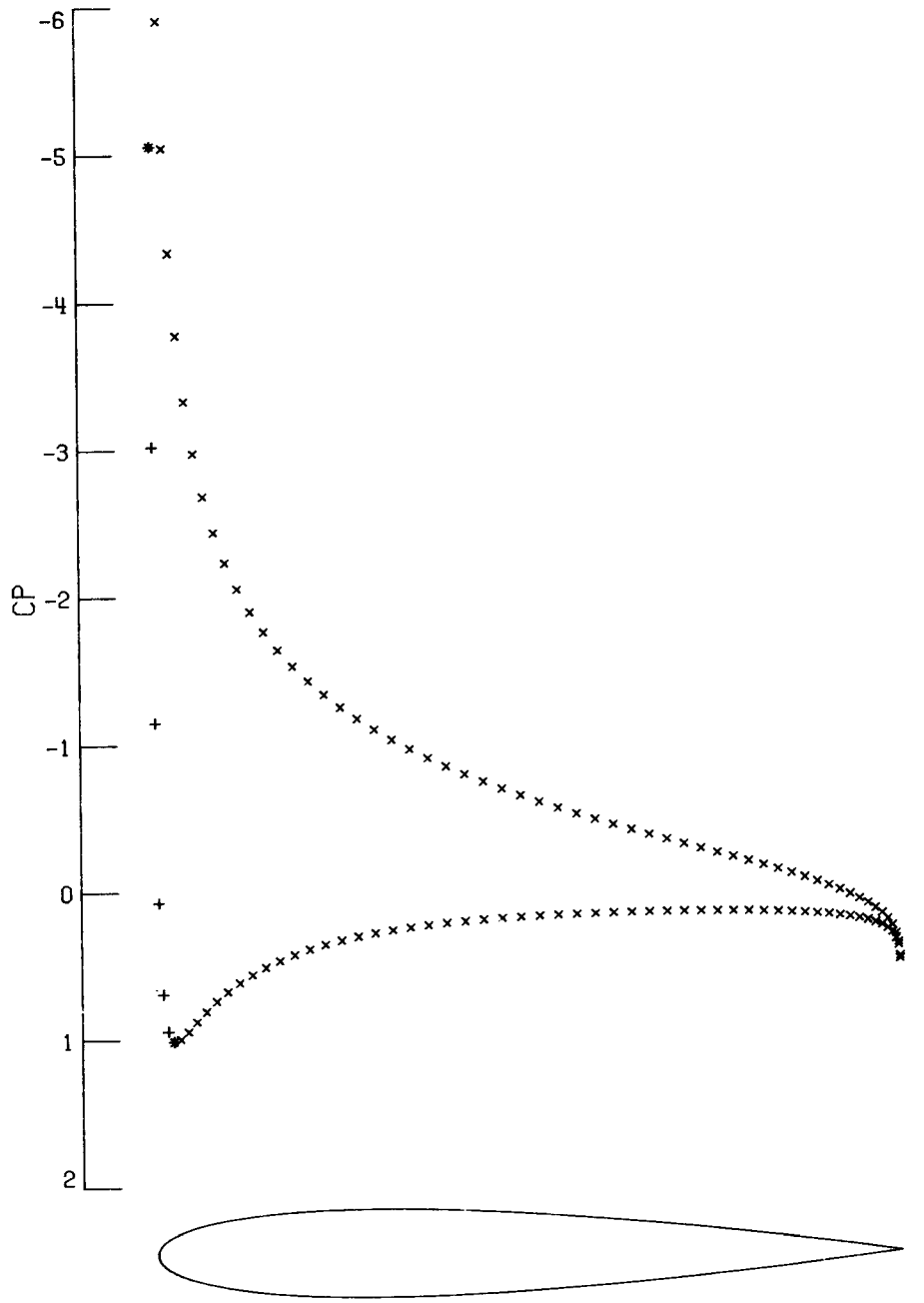

NACA 0012

MACH	.300	ALPHA	10.000		
CL	1.2613	CD	.0026	CM	-.0104
GRID	120X34	NCYC	2000		

(b)

Fig. 6.- Concluded.

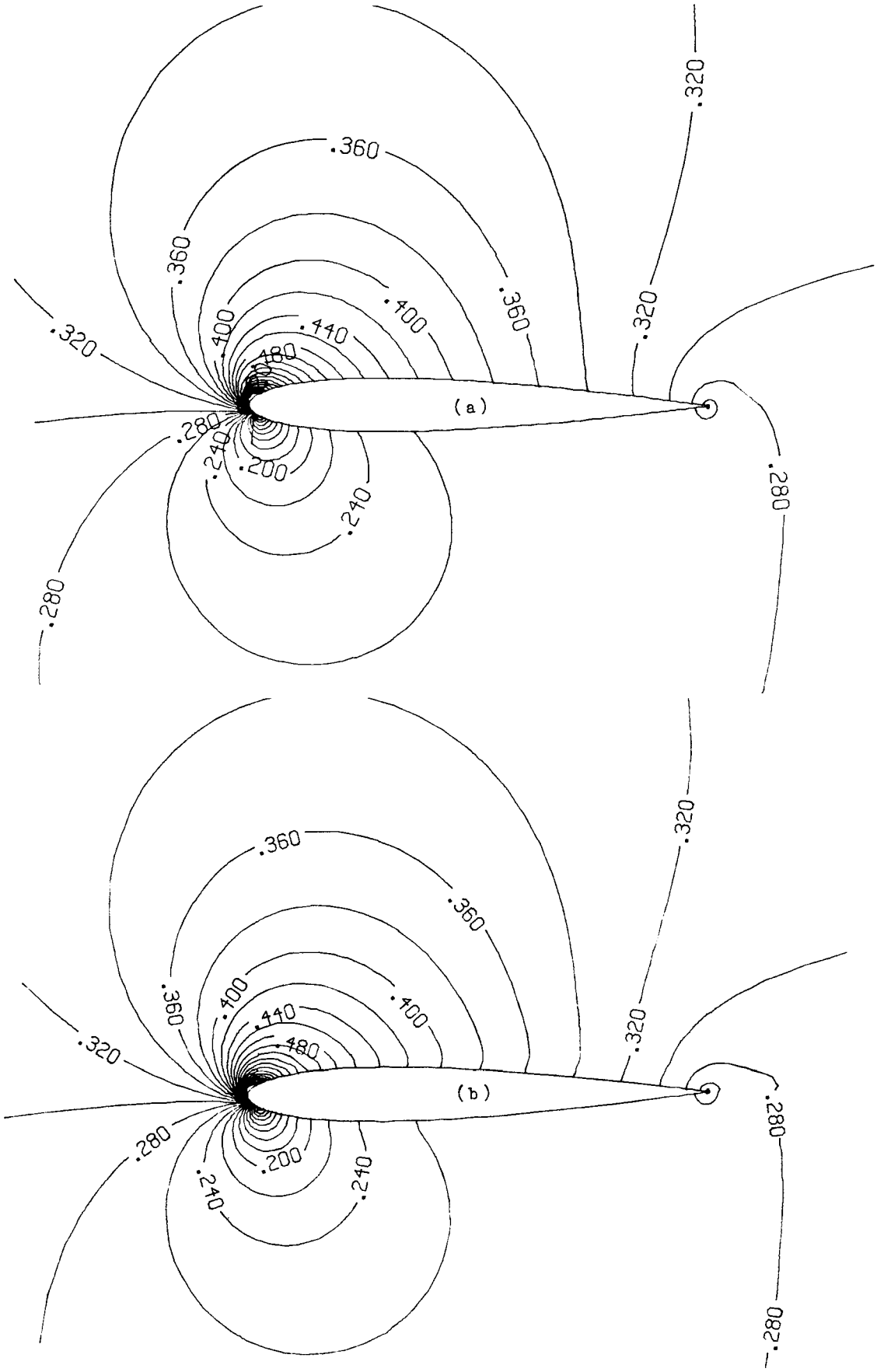

Fig. 7.- Mach number contours computed (a) with FLO 36 and (b) with FLO 52-S.

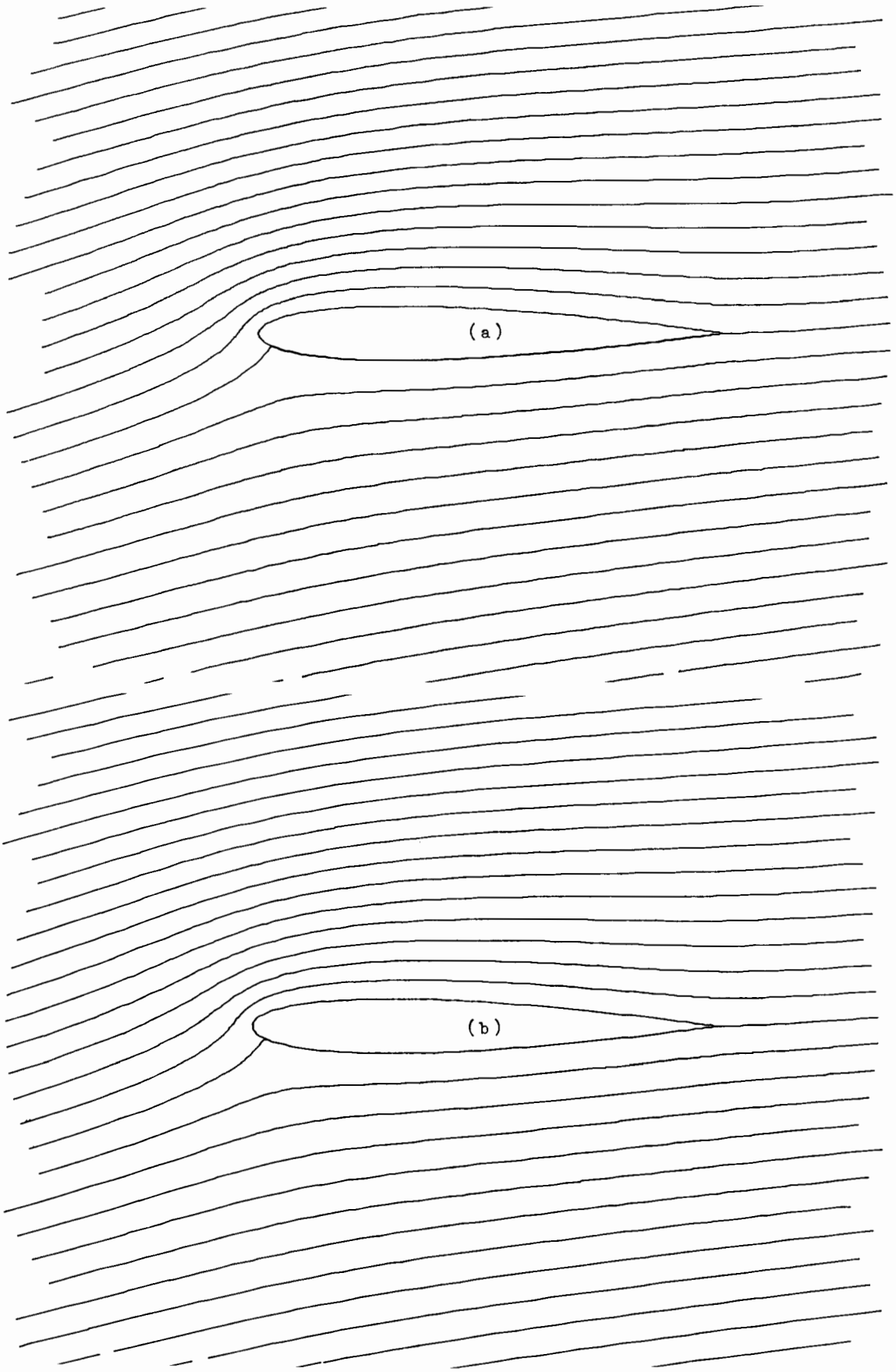

Fig. 8.- Streamline pattern computed (a) with FLO 36 and (b) with FLO 52-S.

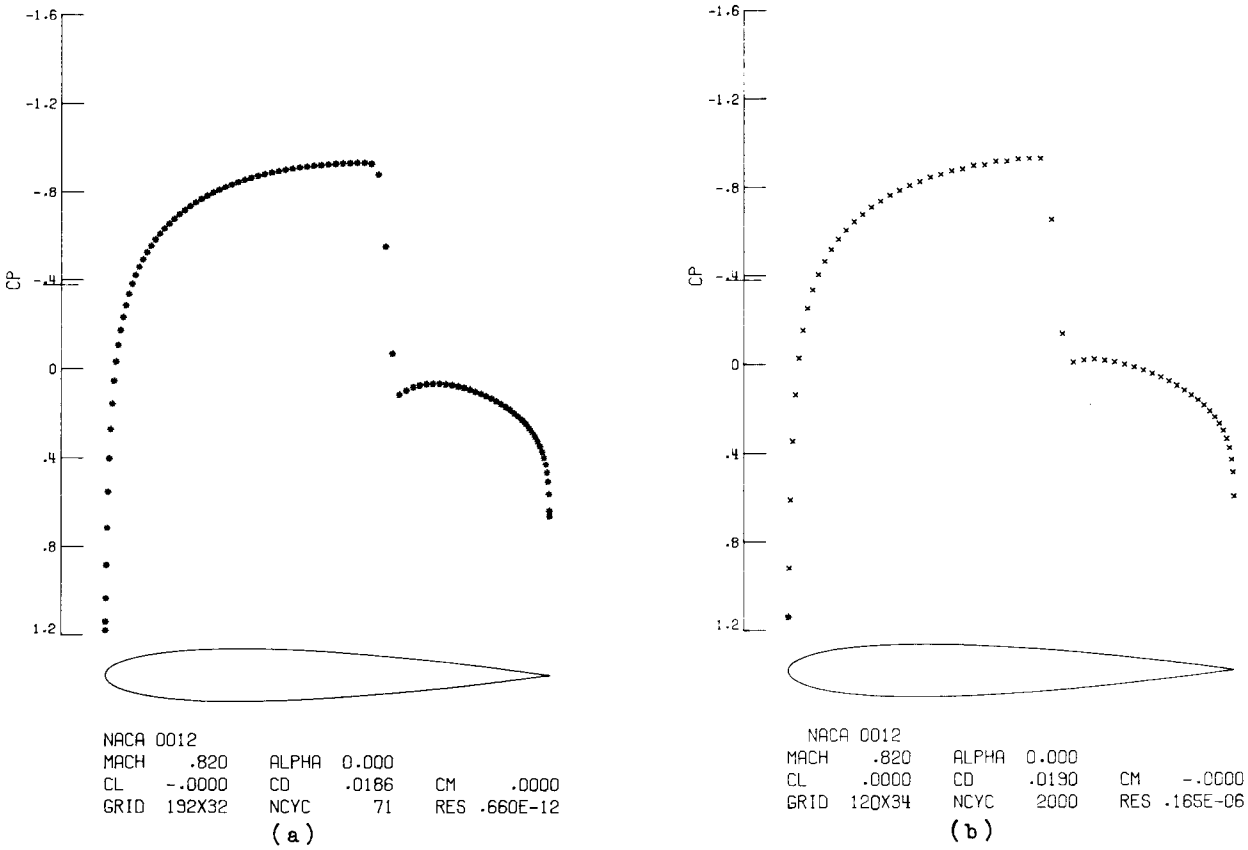

Fig. 9.- Pressure coefficient computed (a) with FLO 36 and (b) with FLO 52-S.

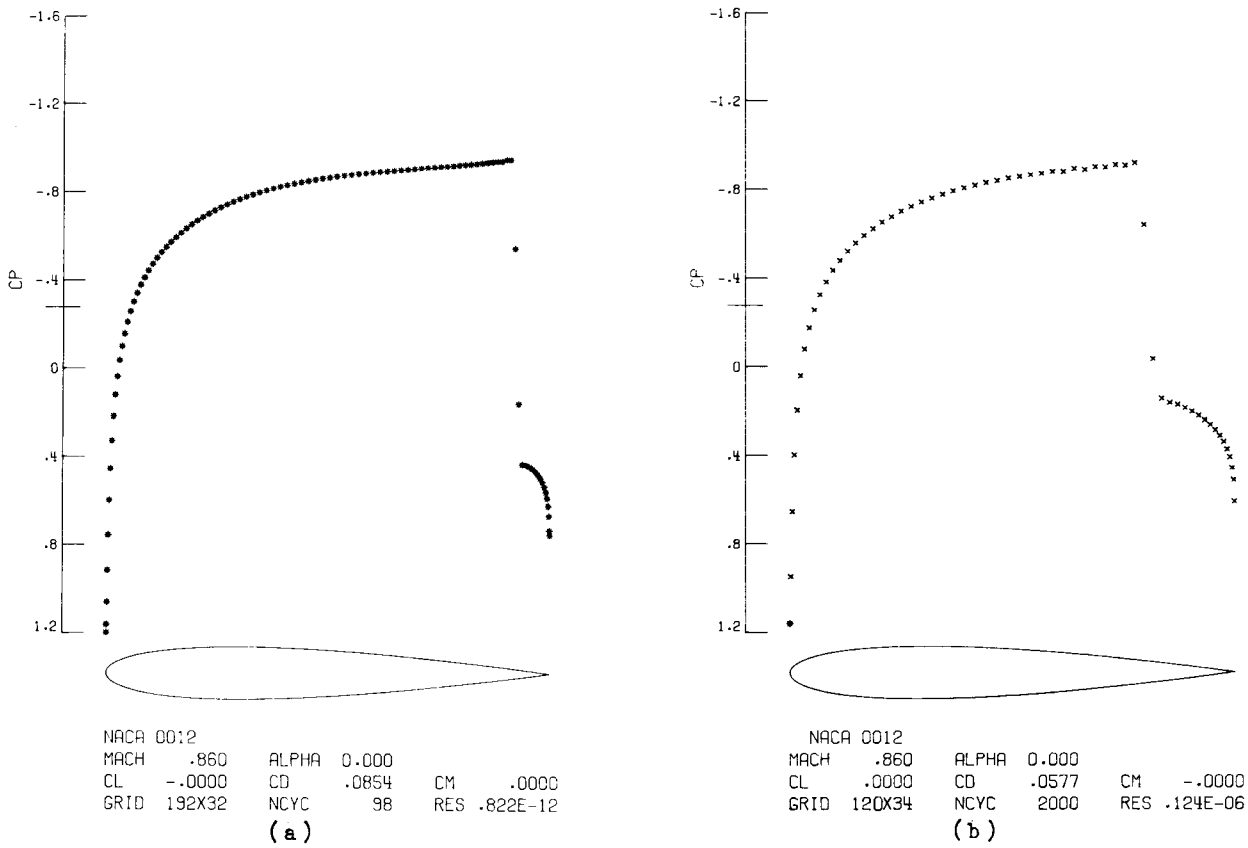

Fig. 10.- Pressure coefficient computed (a) with FLO 36 and (b) with FLO 52-S.

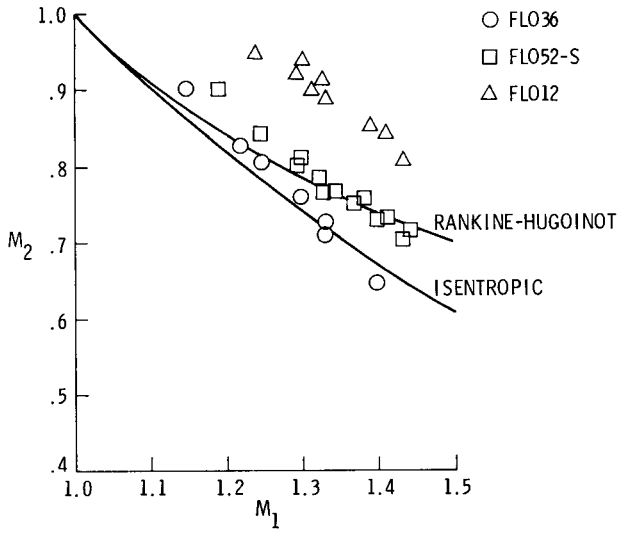

Fig. 11.- Shock jump conditions computed with FLO 36, FLO 12, and FLO 52-S compared to exact jump.

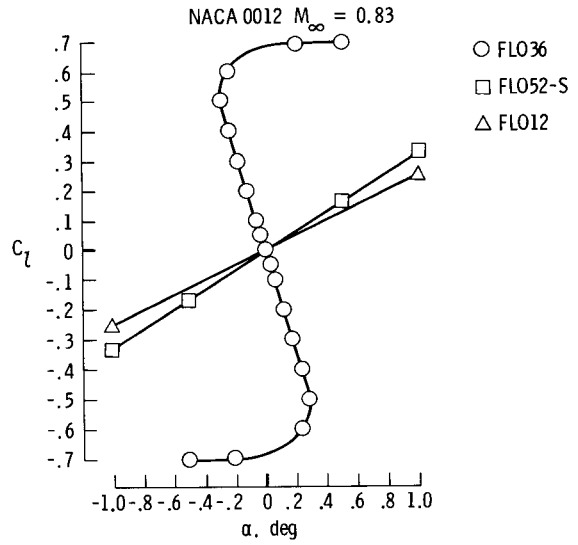

Fig. 12.- Lift-α curve obtained with FLO 36, FLO 12, and FLO 52-S.

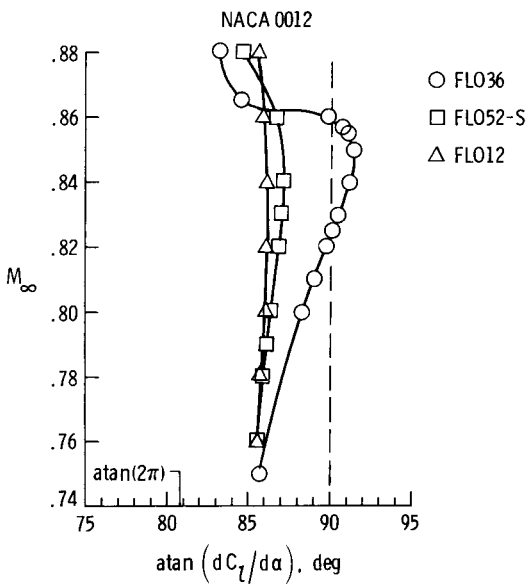

Fig. 13.- Comparison of the angle made by lift-α curve with the abscissa at zero lift at different Mach numbers.

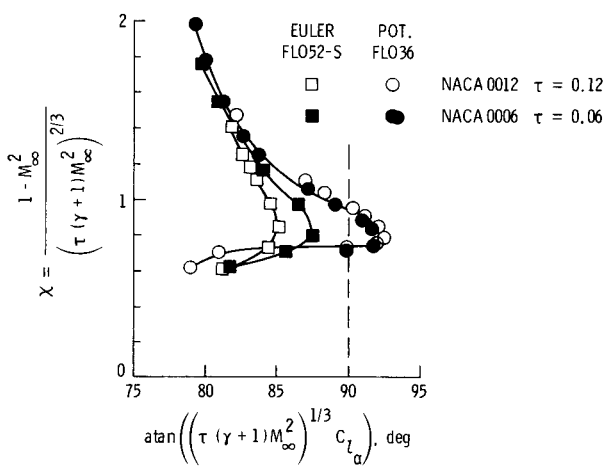

Fig. 14.- Comparison of angle made by lift-α curve in terms of transonic similarity parameters.

END